IEEE Access
Multidisciplinary ⋮ Rapid Review ⋮ Open Access Journal

Received January 3, 2022, accepted February 1, 2022, date of publication February 9, 2022, date of current version February 22, 2022.

Digital Object Identifier 10.1109/ACCESS.2022.3150335

Computational Fluid Dynamics as an Engineering Tool for the Reconstruction of Endovascular Prosthesis Endoleaks

ANDRZEJ POLANCZYK[1], ALEKSANDRA PIECHOTA-POLANCZYK[2], IHOR HUK[3], CHRISTOPH NEUMAYER[3], AND MICHAL STRZELECKI[4]

[1]Faculty of Safety Engineering and Civil Protection, Main School of Fire Service, 01-629 Warsaw, Poland
[2]Department of Medical Biotechnology, Faculty of Biochemistry, Biophysics and Biotechnology, Jagiellonian University, 30-387 Kraków, Poland
[3]Division of Vascular Surgery, Department of Surgery, Medical University of Vienna, 1090 Wien, Austria
[4]Institute of Electronics, Lodz University of Technology, 93-590 Łódź, Poland

Corresponding author: Andrzej Polanczyk (andrzej.polanczyk@gmail.com)

This work involved human subjects or animals in its research. Approval of all ethical and experimental procedures and protocols was granted by the Local Institutional Review Board of the Medical University of Vienna under Application No. 2069/2012.

ABSTRACT Background and objectives: Endovascular prosthesis placement is a predominant surgical procedure to reduce the risk of aneurysm rupture in abdominal aortic aneurysm patients. The formation of an endoleak is a major complication of stent-graft placement. Therefore, the aim of this study was to determine the influence of stent-graft's spatial configuration on the risk of leakage under realistic flow conditions. Materials and Methods: We analyzed data collected from 10 male patients 55 $\pm$ 3 years old after CTA who had undergone endovascular treatment. Computational Fluid Dynamics technique was applied for the reconstruction of blood hemodynamic. Two cases of the stent-graft were analyzed each time, with and without the endoleak, reconstructed from one patient data with the endoleak. Endoleak-free geometries were prepared by virtual closure of the opening. Results: It was observed that high value of the blood velocity around the endoleak may provoke its slowly rupture, which may increase the blood flow to the aneurysm sack in the case of type II endoleaks. Moreover, the appearance of endoleak reduces the average blood velocity in the entire stent-graft which in some cases may contribute to blood coagulation. Furthermore, no clot can form at the site of the endoleak due to the high value of wall shear stress near of the endoleak which prevents thrombosis.

INDEX TERMS Implants, finite element analysis, stress, structural shapes, biomedical imaging, leak detection, computational modeling, medical simulation, Doppler measurement, surgical instruments.

I. INTRODUCTION

Abdominal aortic aneurysm (AAA) is a major problem of morbidity and mortality [1]. To prevent sudden aneurysm rupture, the mean enlargement rate and the occurrence of sudden change in the size of AAA are also important check points for subsequent follow-up medical care [2]. One of the methods for the reconstruction of proper blood flow in patients with AAA is implantation of endovascular prosthesis (stent-graft) in the area of wall dissection or aortic aneurysm [3]. Although endovascular prosthesis implementation has numerous benefits, it may have some negative clinical outcome over time [4]. The complexity of hemodynamics in the aortic aneurysm region may indicate several complications in patients after stent-graft placement e.g., an aneurysm expansion and rupture or blood seepage into the cavity between the aneurysm's wall and the stent-graft's wall. The most common post-operative complications in endovascular repair are endoleaks i.e., persistence of blood flow into the aneurysm sac after device placement [5]. Endoleaks are defined as continued perfusion of the aneurysm sac despite endovascular aortic repair [6]. Moreover, endoleaks can be classified according to their temporal nature (type I endoleaks - poor apposition of the device to the aortic wall; type II endoleaks - reverse flow into the aneurysm sac from aortic branch vessels such

The associate editor coordinating the review of this manuscript and approving it for publication was Kin Fong Lei.

as the inferior mesenteric artery or lumbar arteries; type III endoleaks - a defect in the fabric of the graft, such as a tear resulting from a fractured stent, or due to separation of the modular components of the endograft and type IV endoleaks - filtration of plasma through the fabric of the graft) [7]. Therefore, AAA size and its spatial configuration have to be assessed to select a proper type of a stent-graft before its implantation [8]. Furthermore, initial diagnosis require the assessment of the diameter of the aorta below, above and at the level of the renal arteries, the diameter of aneurysm sac, and the diameter of common and external iliac arteries [9].

Medical imaging techniques allow to evaluate the morphology of the AAA [10]. Routine studies, e.g., an electrocardiography (ECG) or chest x-ray, may help differentiate the other possible causes of chest pain; however, they may also be misleading [11]. A prompt diagnosis based on the early suspicion is mandatory for successful treatment. However, the quickest and most accurate method to confirm such diagnosis is CT scanning of the AAA [12]. The sensitivity and specificity of CT are excellent, but in patients with poor renal function or allergy to iodinated dye, CT angiography is questionable, and other imaging modalities such as magnetic resonance imaging (MRI) or ultrasonography should be considered instead [13]. However, none of the medical imaging applications allow to predict the hemodynamic effect of the surgical intervention [14]. The current in-hospital mortality rates remain significant, at the level of approximately 10% [15]. For this reason, computational cardiovascular mechanics has allowed scientists to create complex 3D models for the simulation of cardiovascular pathologies [16]. Therefore, numerical methods for solving issues related to blood flow in vessels are widely applied [17]. Computational Fluid Dynamics (CFD) method is a useful engineering tool for hemodynamic analysis [18] and different mathematical tools are being applied, i.e. Ansys software, Adina software, and OpeanFOAM software, for blood flow reconstruction [19]–[21]. CFD simulations based on patient-specific models may provide insight into the biomechanical behavior of blood flow, allowing quantitative analysis of hemodynamic patterns, and predicting clinical progression. However, its clinical value still requires verification [22]. Depending on the type of problem analyzed, blood maybe reconstructed as Newtonian or non-Newtonian [23]. Such approach enables assessment of the diseases severity and improves planning of the reconstructive surgery [24]. Moreover, application of computational methods allows considering of different mechanical and fluid parameters, e.g., wall shear stress (WSS) [25]. Additionally, in our previous research we focused on the estimation of how stent-graft's geometry impacts the WSS value after stent-grafting [8]. Also, we investigated the impact of particular stent-graft parts on the thrombus formation in terms of the optimization of the spatial configuration of the endovascular prosthesis [3]. Therefore, the aim of this study was to determine the influence of stent-graft's spatial configuration on the risk of leakage under realistic conditions of the blood flow.

TABLE 1. Dimensions of implanted stent-graft's.

Patient	Main body diameter [mm]	Iliac leg diameter Left/Right [mm]
P1	28	10/12
P2	30	12/14
P3	28	12/12
P4	28	10/12
P5	30	12/14
P6	28	12/14
P7	28	12/12
P8	30	12/14
P9	30	12/12
P10	30	12/14

This paper is organized as follows: In Section II (2. Materials and Methods), medical data and a mathematical model with boundary conditions and its verification is described. Section III (3. Results) presents the results directed in the computer simulation. In Section IV (4. Discussion), a discussion is proposed, while section V (5. Conclusions) concludes the paper.

II. MATERIAL AND METHODS

A. MEDICAL DATA

In this study we used data collected from 10 male patients 55 ± 3 years old after CT angiography (512 × 512 × 270 voxels, in-plane resolution of 0.78 × 0.78 mm, slice thickness 1 mm) (Figure 1) (GE Light-Speed 64 VCT; GE Healthcare, Fairfield, CT, USA) and USG-Doppler (GE Vivid 7, GE Healthcare, USA), who underwent endovascular treatment at the Medical University of Vienna between 2012–2015. Patients were implanted with stent-graft Zenith (Table 1) made by COOK (Cook Medical, USA). The scaffold of Zenith stent-graft is made of openwork metal segments which do not overlap, and the cover is made of Dacron. Patients' data were retrospectively collected after obtaining written informed consent to participate in the study. Medical data and images were anonymized by coding information before access and analysis. The study was approved by the local Institutional Review Board (2069/2012) of the Medical University of Vienna.

With the use of Digital Imaging and Communications in Medicine (DICOM) data, patient-specific 3D computer models of the patients' endovascular prothesis placed in AAA were created as previously described [26].

In each case the inlet to the system was just below the mesenteric artery outlet and the outlets were in the femoral arteries at the level below the stent-graft ending. To compare two cases of the stent-graft, with and without the endoleak, data from one patient with the endoleak was used. We started with preparation of the stent-graft with type II endoleak observed in upper part of the prosthesis (Figure 2a). Then the endoleak was virtually closed (Figure 2b). This operation enabled us to show the differences in blood hemodynamic for the same patient for the two cases.

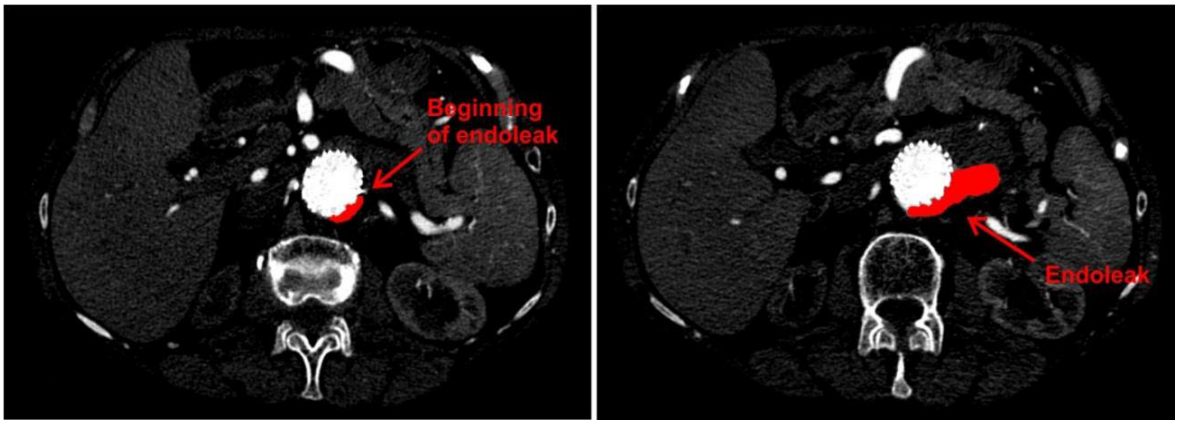

FIGURE 1. CT slices with an endoleaks for an exemplary patient. The endoleak was marked with red color.

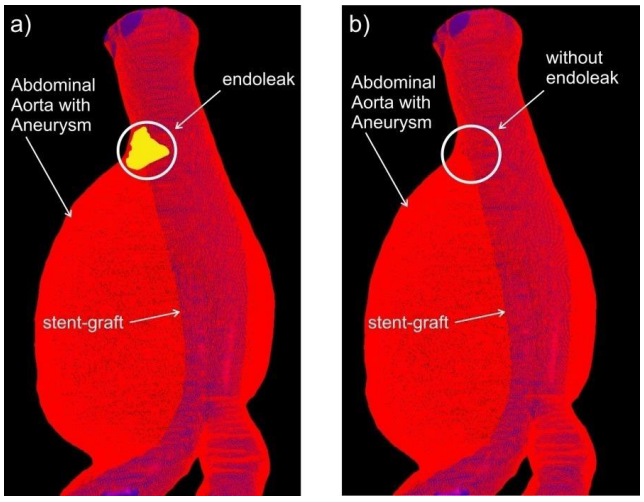

FIGURE 2. The three-dimensional reconstruction of a stent-graft a) with an endoleak, b) without an endoleak.

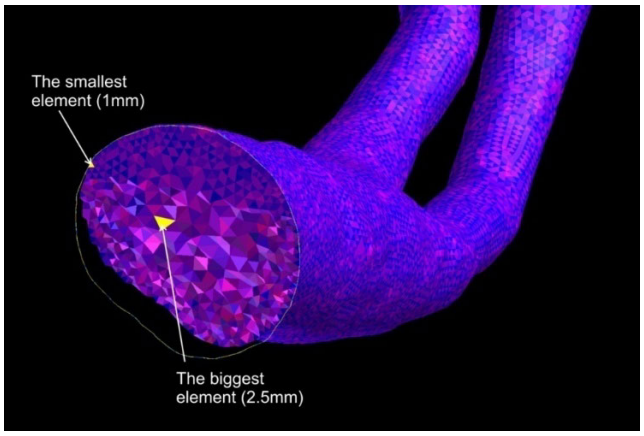

FIGURE 3. The size of mesh elements inside the analyzed endovascular prosthesis model.

B. MATHEMATICAL MODEL

The ANSYS ICEM CFD (ANSYS, Canonsburg, PA USA) software was used to discretize the analyzed object. Volume meshing with tetrahedral elements type T-Grid was applied [27]. The size of elements ranges from 1 to 2.5 mm

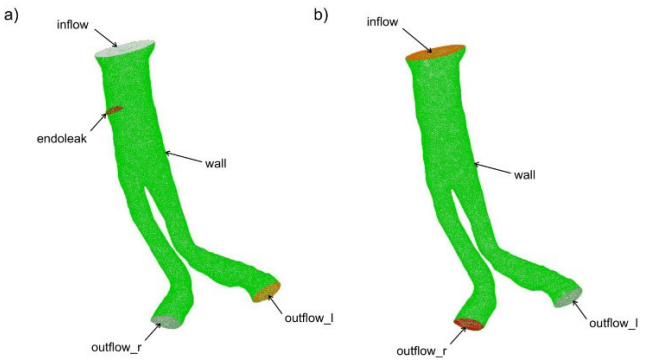

FIGURE 4. Boundary types for the stent-graft a) with the endoleak, b) without the endoleak.

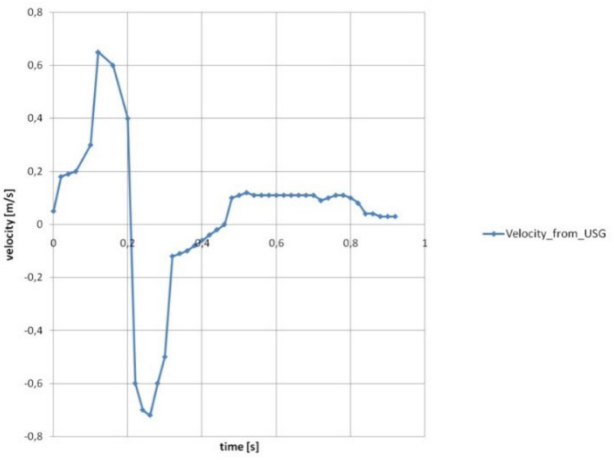

FIGURE 5. Profile of blood velocity at the inlet of the stent-graft from USG research.

(Figure 3). The number of tetrahedral mesh elements for areas depended on individual geometry and changed from approximately 350 000 to 500 000. Moreover, according to mesh independent test as well as following Sun *et al.* approach the number of the boundary layer was set to 5 [28].

The CFD simulations were carried out with ANSYS FLUENT 18.2 software (ANSYS, Canonsburg, PA, USA) as previously described in [29]. Depending on the analyzed

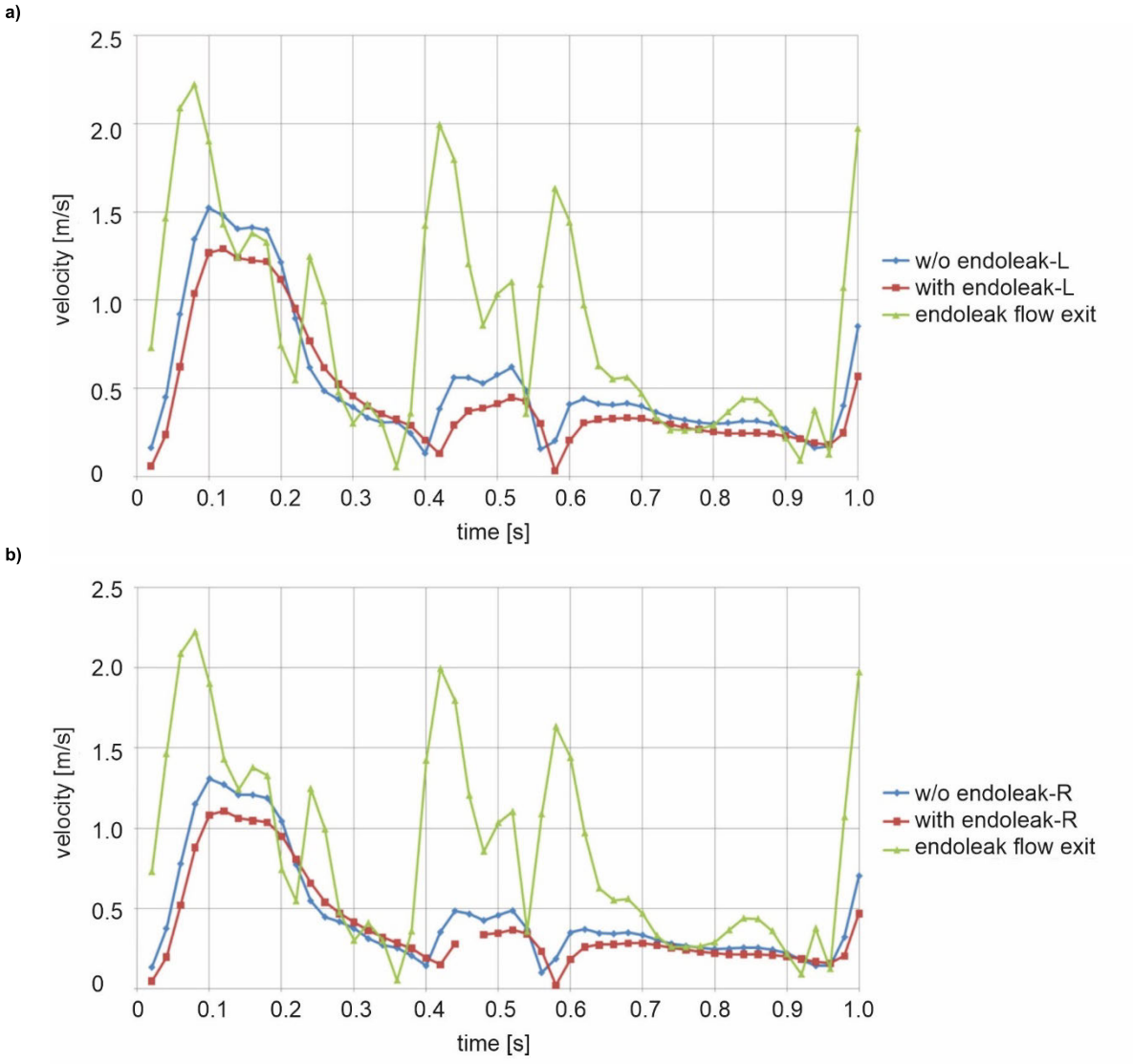

FIGURE 6. An example of velocity curves for a) the left outlet of stent-graft's bifurcated part without the endoleaks (w/o endoleaks-L), with the endoleaks (with endoleaks-L) and endoleaks flow exit (endoleak flow exit), b) the right outlet of stent-graft's bifurcated part without the endoleaks (w/o endoleaks-R), with the endoleaks (with endoleaks-R) and endoleaks flow exit (endoleak flow exit).

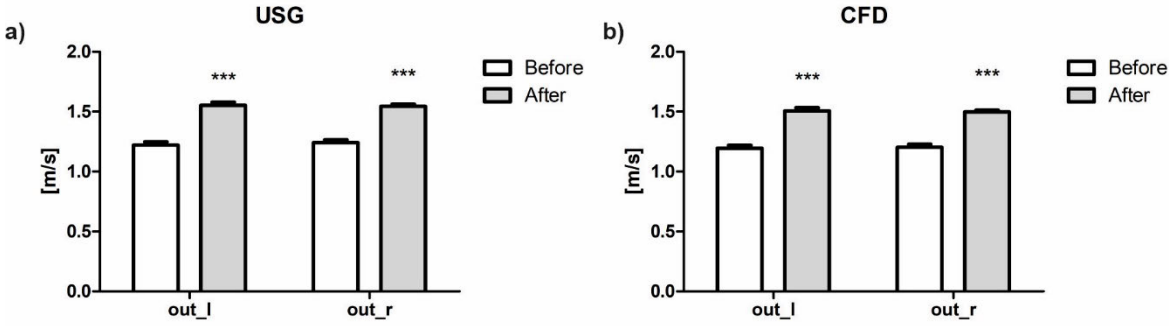

FIGURE 7. Change of the blood velocity in the left and right limb of endovascular prosthesis for the stent-grafts with endoleaks (before) and after virtual closure of endoleaks (after). Panel (a) is for USG-Doppler data and panel (b) is for CFD results. Mean ± S. E.M. Statistical analysis made with 2-way ANOVA; *** - $p < 0.001$ – statistically significant difference between velocities before and after.

stent-graft, with or without the endoleak, there were different boundary types: (1) the one inlet and three outlets of the blood (including two iliac arteries and one endoleak) (Figure 4a) had a stent-graft with the endoleak, and (2) the one inlet and

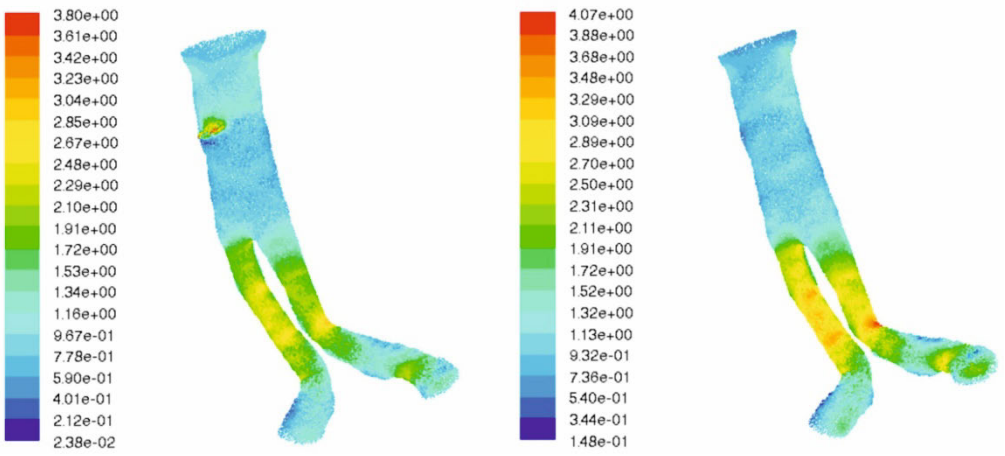

FIGURE 8. An example of the blood velocity distribution for the longitudinal stent-graft with and without the endoleak for time step 0.08s, (m/s).

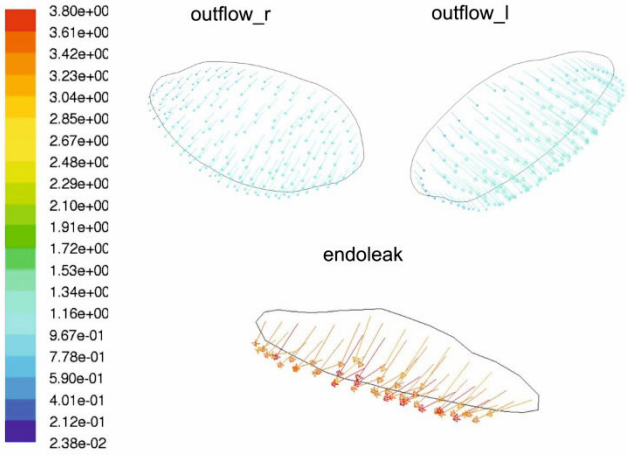

FIGURE 9. An example of velocity distribution for both outflows of both bifurcated part of the stent-graft and for the endoleak (time step 0.08s).

two outlets of the blood (Figure 4b) had a stent-graft without the endoleak.

Each time, at the inlet to the stent-graft, pulsating character of blood flow as in the real human vascular system, based on the use USG-Doppler examination (Figure 5), was applied which was in line with Li and Kleinstreuer [30]. Basing on these data we defined a pulsating profile of the blood using a Fourier series.

The calculated blood flow profile covers 1 second. It includes slightly over 1 cycle of heart's beat. The 1 second of calculations contains all 4 steps of heart cycle, isovolumetric contraction (tenser about 0.05 s), isotonic contraction (throw about 0.25 s), isovolumetric contraction (looseness about 0.10 s), isotonic contraction (fulfillment about 0.40 s). Moreover, the blood flow profile was extracted from ten consecutive cycles, each of which took 1 s. Then, the three first cycles were excluded as described by Tyfa *et al.* [18]. Moreover, it was assumed that the patients who were subjected to USG-Doppler were in the resting state. Therefore, 1 s period was a representative time, which comprised one whole heart cycle and reflected basal conditions in a patient. Furthermore, the character of blood flow at the inlet of the stent-graft was assumed as a laminar flow [21], [31]. To reconstruct the real rheological properties of blood it was treated as a non-Newtonian liquid. Self-made algorithm, in which viscosity η is a function of shear velocity and hematocrit (Hct) value, was applied [23]. The density of blood was assumed as a constant value of 1050 kg/m^3. The mathematical domain was described with the boundary conditions as follow: at the inlet, an assumed condition of blood flow velocity was $\boldsymbol{u} = (u, v, w)$, while at the outlets the condition p = const was taken [21].

Calculation of 1 second of the blood flow profile, with previously described boundary conditions, lasted 30-72 hours depending on the analyzed case. The simulations were carried out with Intel Core 2 Quad 2.5 GHz, 8 GB RAM.

C. MATHEMATICAL MODEL VERIFICATION

Each time the blood velocity from CFD simulation for the outflows for the patient was compared to data from USG-Doppler. Statistical analysis was performed using Statistica 12.0 software (Statsoft). Values were presented as mean ± S.E. (standard error). Comparisons between endoleak and without endoleak cases were made using the 2-way ANOVA test after verifying normality and variance. Data were considered significantly different when $p < 0.05$ unless otherwise noted. Moreover, Bland-Altman plots were used to analyze the agreement between USG-Doppler and CFD data.

III. RESULTS

Reconstruction of blood flow through the stent-graft placed in the AAA allowed description of the blood velocity, static and dynamic pressure and wall shear stress distribution for all analyzed patients and cases.

A. BLOOD VELOCITY

For each of the analyzed patients, the blood velocity profiles at the outlets of the bifurcated part of the stent-graft differed

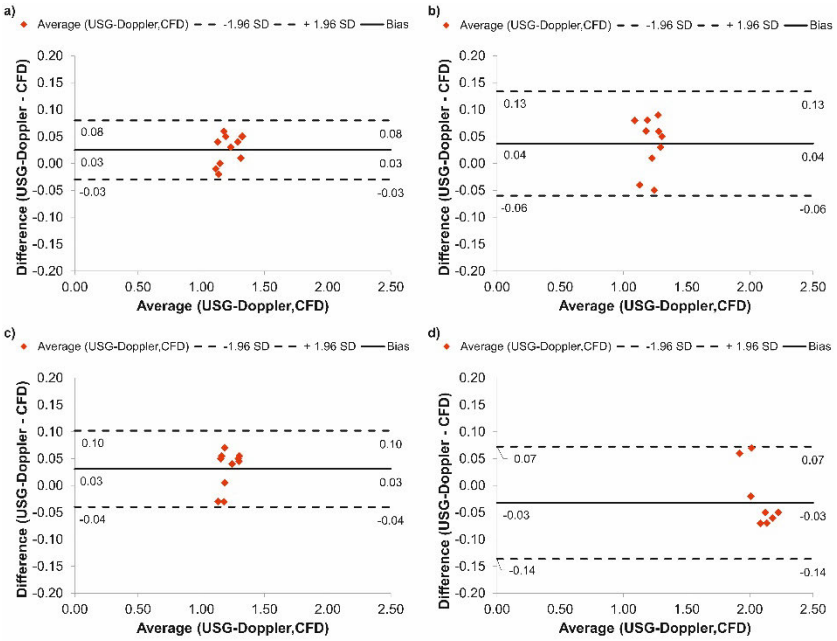

FIGURE 10. Comparison of the blood velocity from CFD and USG-Doppler for (a) the left outflow of stent-graft, (b) the right outflow of stent-graft, (c) the average outflow of stent-graft, (d) the leak outflow of stent-graft.

in both cases (with and without endoleaks). It was observed that blood velocity on the outlets of endovascular prostheses without the endoleak (Figure 6a) was higher compared to the endoleak area (Figure 6b). The average blood velocity for the endoleak was about 2 times higher compared to the blood velocity at outlets of the stent-graft (2.09 ± 0.07 m/s and 1.23 ± 0.07 m/s, respectively; according to the 2-way ANOVA, $p < 0.0001$).

The difference in blood velocity results calculated at outlets separately for CFD and USG-Doppler, was in the range of 1% to 4%, with mean value equal to 3%, for the cases with and without endoleak. It was observed that the average value of blood velocity from USG-Doppler in the endoleak was 2.09 ± 0.07m/s, while for the outlets area for the case with endoleak average blood velocity was equal to 1.22 ± 0.09m/s (left branch) and 1.24 ± 0.08m/s (right branch) (Figure 7a). Furthermore, for the case without endoleak the average blood velocity was equal to 1.55 ± 0.08m/s (left branch) and 1.54 ± 0.06m/s (right branch) (Figure 7a). Meanwhile, CFD results indicated that the average value of blood velocity in the endoleak amounts 2.12 ± 0.12m/s, while for the outlets area for the case with endoleak the average blood velocity was equal to 1.20 ± 0.07m/s (left branch) and 1.20 ± 0.08m/s (right branch) (Figure 7b). Additionally, for the case without endoleak the average blood velocity was equal to 1.51 ± 0.08m/s (left branch) and 1.50 ± 0.05m/s (right branch) (Figure 7b). Moreover, the blood velocity distribution indicated that for calculation time equal to 1 second, value of velocity in the endoleak was higher than in the whole stent-graft. Furthermore, blood velocity vectors each time for the longitudinal stent-graft showed that higher values of velocity in the whole investigated domain were noticed in the cases without the endoleak (Figure 8). Prostheses with the endoleak expressed higher velocity only in the area of endoleak, while in the remaining part it was smaller than for the case without the endoleak.

Further comparison of cross-sections in endoleak and both outflows for the bifurcated part of the stent-graft with and without the endoleak, showed differences in blood velocity profiles depicted in Figure 9. The flatter profile of blood velocity was observed in the outlets compared to the endoleak area which profile was rugged. Color of arrows in Figure 9 indicate higher blood velocity of the area of the endoleak compared to the bifurcated outflows. Irregular shape of velocity profile of the endoleak may be provoked be small size of the outflow and pulsating character of blood flow inside of the investigated stent-grafts.

Analysis of all geometries indicated that the Reynolds number in the whole endovascular prosthesis for both cases, with and without the endoleak, was in a range of laminar flow and was smaller than 2100. The highest value of Reynolds was always observed for the endoleak area where it was not higher than 470, as well as for the bend area where it did not exceed 440.

The Bland-Altman analysis showed that there was almost no difference between numerical (CFD) and clinical data (USG-Doppler) regarding blood velocity for the left outflow of stent-graft (0.03 m/s; the length of limits of agreement equal to 0.11 m/s) (Figure 10a), the right outflow of stent-graft (0.04 m/s; length of limits of agreement equal to 0.19 m/s) (Figure 10b), the average outflow (0.03 m/s; length of limits of agreement equal to 0.14 m/s) (Figure 10c), and

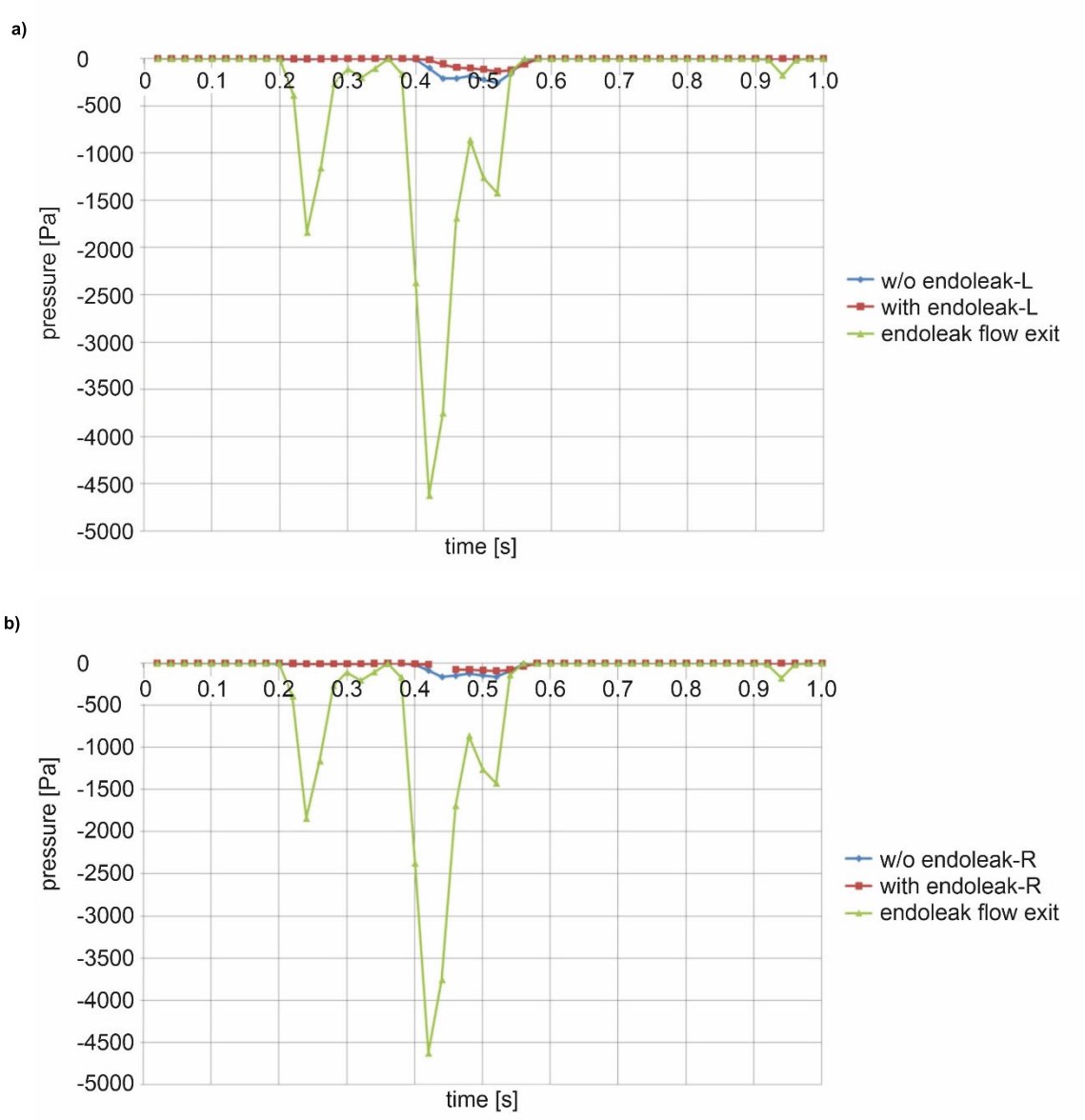

FIGURE 11. An example of the static pressure curves for a) the left outlet of stent-graft's bifurcated part without the endoleaks (w/o endoleaks-L), with the endoleaks (with endoleaks-L) and endoleaks flow exit (endoleak flow exit), b) the right outlet of stent-graft's bifurcated part without the endoleaks (w/o endoleaks-R), with the endoleaks (with endoleaks-R) and endoleaks flow exit (endoleak flow exit).

the leak area (0.03 m/s; length of limits of agreement equal to 0.21 m/s) (Figure 10d).

B. BLOOD PRESSURE

The value of the static and dynamic pressure in the investigated stent-grafts evolved for every time step of calculations. The value of the static pressure for both outlets was always different due to the difference in diameters of bifurcation.

We observed that during one second which referred to one whole cardiac cycle, the minimal average static pressure for the left outflow was equal to -260 ± 11Pa, while the maximal average static pressure was 0Pa (Figure 11a). For the right outflow, the minimal average static pressure was equal to -150 ± 8Pa, and the maximal average static pressure was equal to 0Pa (Figure 11b). The same tendency was observed for the stent-grafts with the endoleak; however, the value of static pressure for outflows of bifurcated part was lower compared to the case without endoleak. Meanwhile, the minimal average static pressure for the endoleak was equal to -4600 ± 44Pa, while the maximal average static pressure was 0Pa.

The static pressure changes exerted by the blood flow on the wall was shown in Figure 12. Different color bands represent different level of static pressure and give an idea of pressure gradient distribution along the wall. Each time contours of static pressure for the longitudinal stent-graft showed that the highest value appeared at the stent-graft's

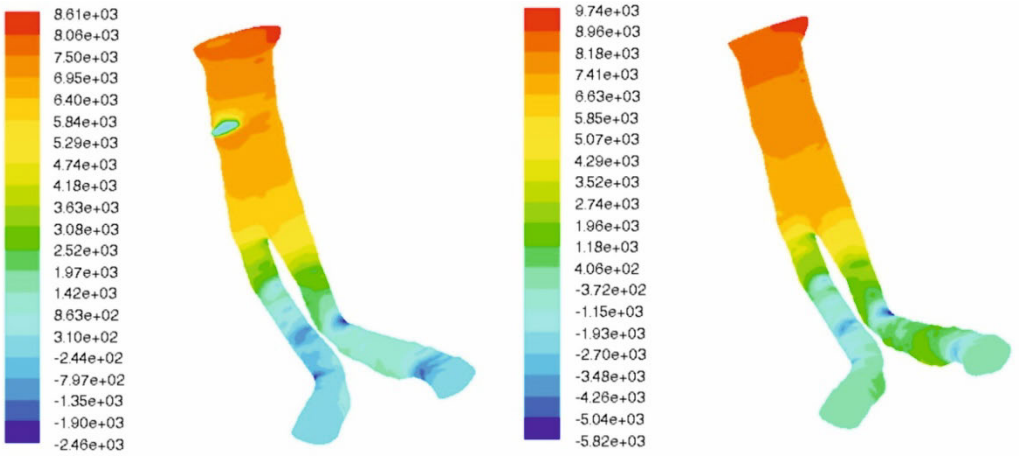

FIGURE 12. An example of static pressure changes for the longitudinal stent-graft with and without the endoleak for time step 0.08s, (Pa).

a)

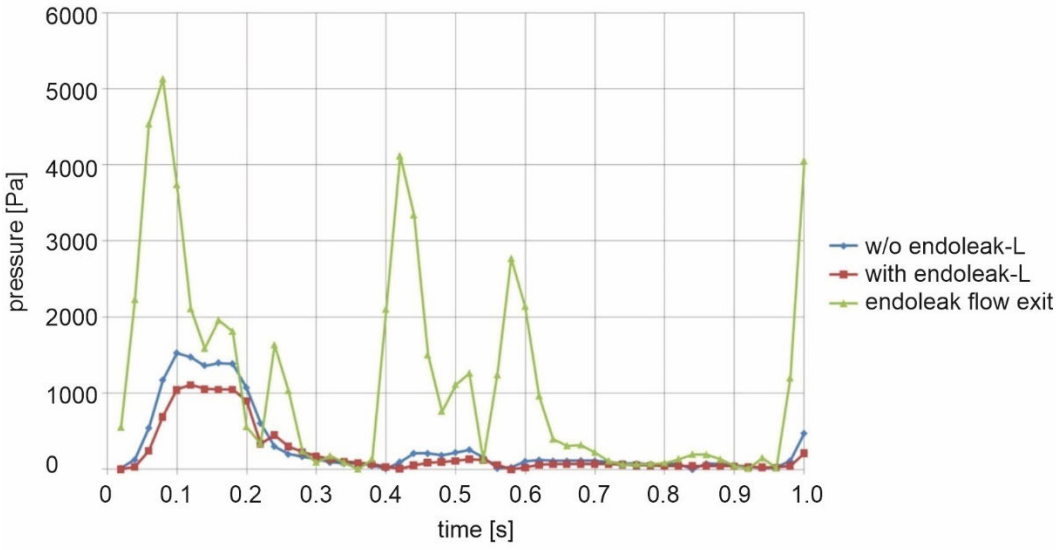

b)

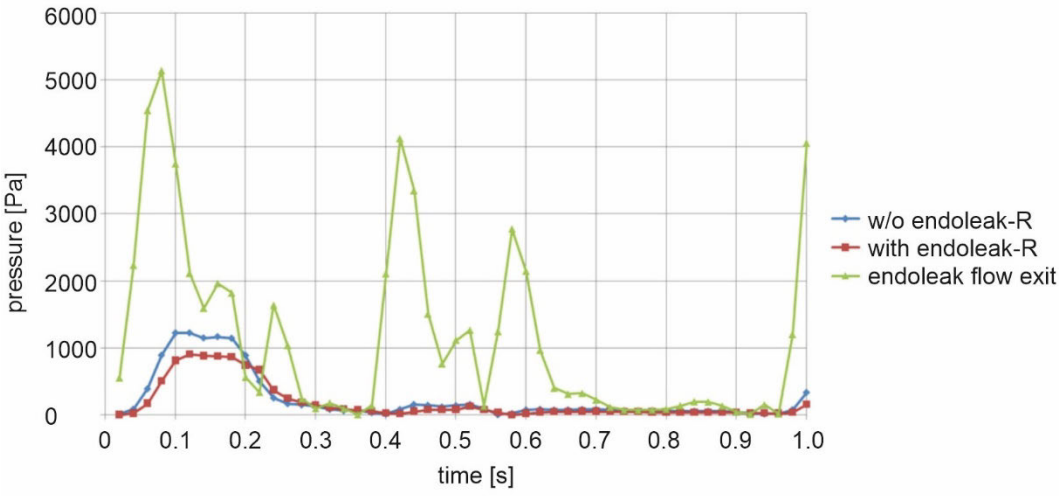

FIGURE 13. An example of dynamic pressure curves for a) the left outlet of the stent-graft's bifurcated part without the endoleaks (w/o endoleaks-L), with the endoleaks (with endoleaks-L) and endoleaks flow exit (endoleak flow exit), b) the right outlet of stent-graft's bifurcated part without the endoleaks (w/o endoleaks-R), with the endoleaks (with endoleaks-R) and endoleaks flow exit (endoleak flow exit).

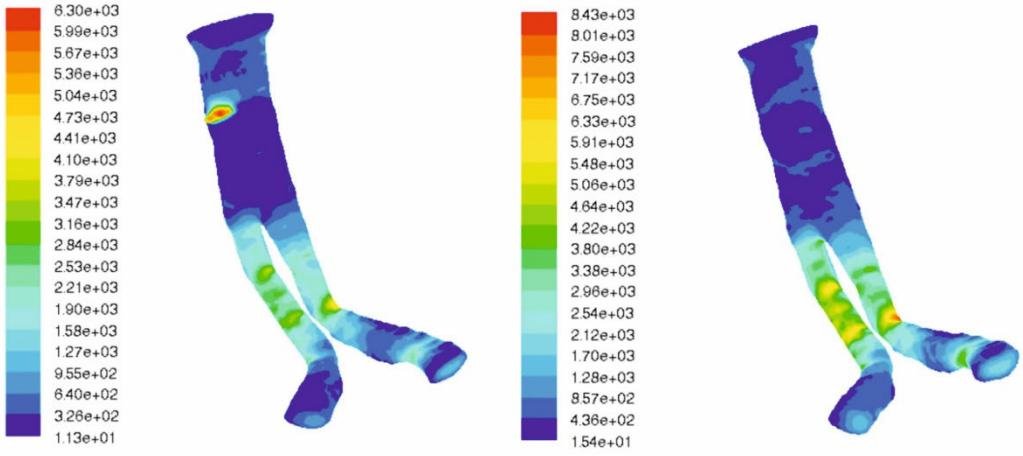

FIGURE 14. An example of dynamic pressure for the longitudinal stent-graft with and without the endoleak for time step 0.08s.

a)

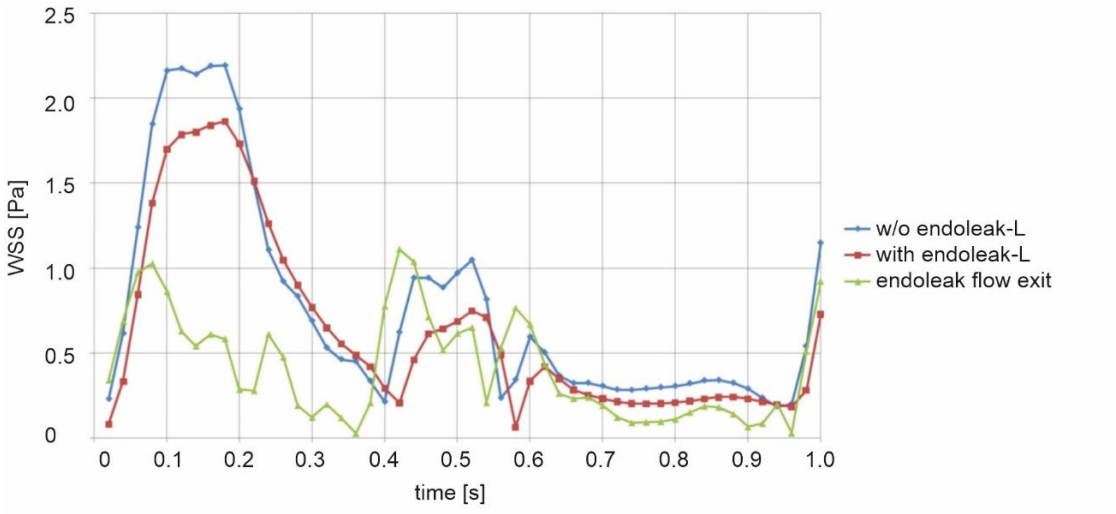

b)

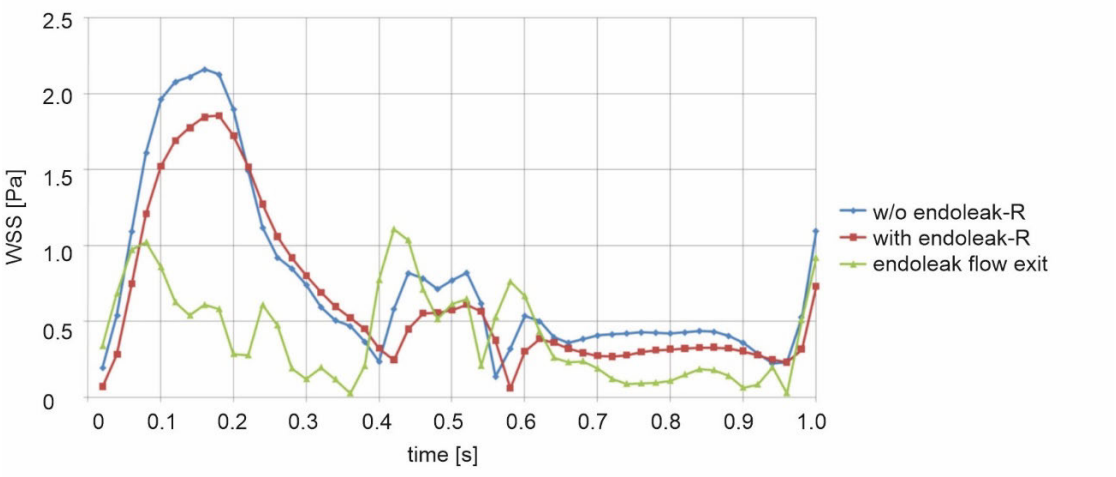

FIGURE 15. An example of wall shear stress curves for a) the left outlet of stent-graft's bifurcated part without the endoleaks (w/o endoleaks-L), with the endoleaks (with endoleaks-L) and endoleaks flow exit (endoleak flow exit), b) the right outlet of stent-graft's bifurcated part without the endoleaks (w/o endoleaks-R), with the endoleaks (with endoleaks-R) and endoleaks flow exit (endoleak flow exit).

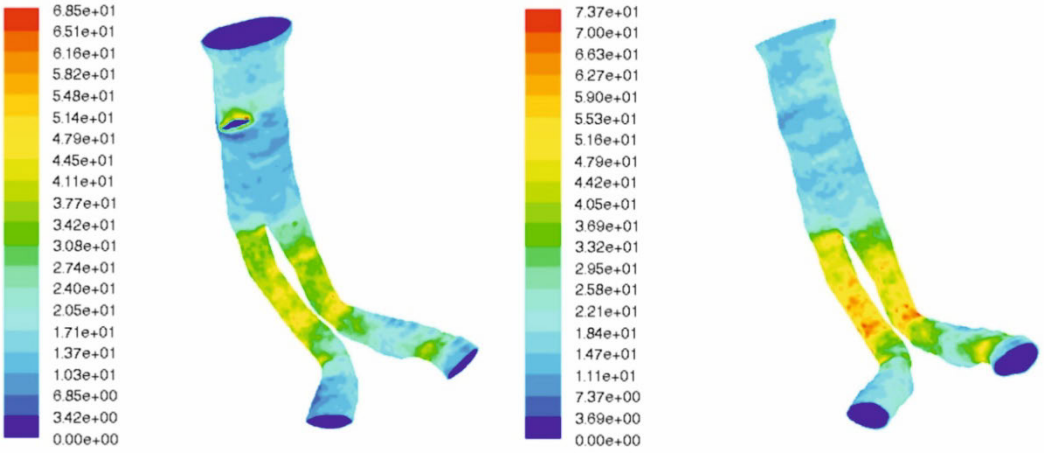

FIGURE 16. An example of wall shear stress for the longitudinal stent-graft with and without the endoleak for time step 0.08s.

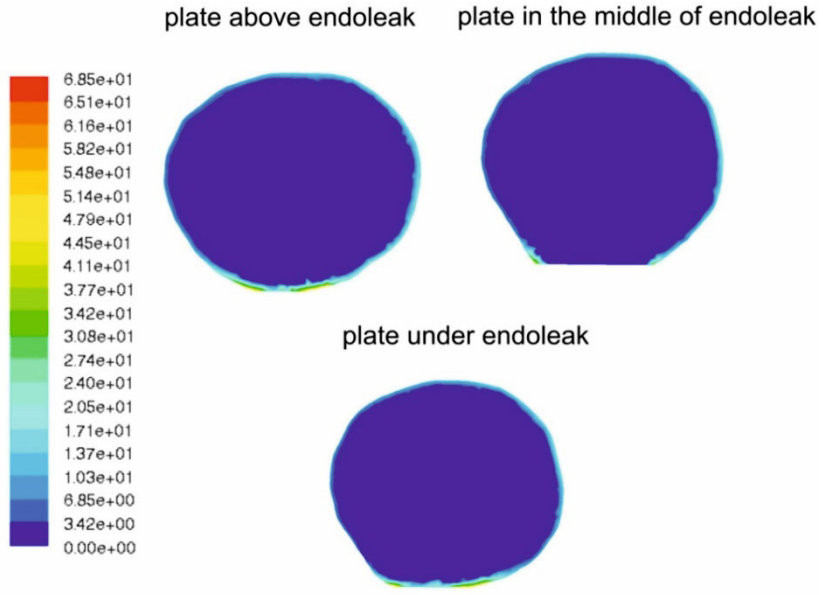

FIGURE 17. An example of cross-sections representing wall shear stress on the stent-graft's wall over, in the middle and under the endoleak for time step 0.08s.

inlet. Also, with increasing time step static pressure decreased in places with higher blood velocity. Depending on the case, the value of average static pressure was 9293 ± 24Pa for the stent-grafts without the endoleak and it decreased to 7288 ± 73Pa for the case with the endoleaks.

The value of dynamic pressure was higher for prostheses without the endoleak. It was related to appearence of higher blood velocity in the stent-grafts without the endoleak. During a time period of 1 second of calculations time, the average velocity in the endoleak was several times higher than in the outflows of the stent-graft's bifurcated part with and without the endoleak.

The highest average value of dynamic pressure for the endoleak was 5150 ± 21Pa (Figure 13a and Figure 13b). For outflows it depended on the leg of bifurcation and amounts for the left leg 1050 ± 12Pa with the endoleak and 1550 ± 16Pa for the other. The same tendency of decreasing pressure for the stent-grafts with the endoleak was observed each time for the right leg of bifurcation where the average value of dynamic pressure was 900 ± 11Pa with the endoleak and 1200 ± 18Pa without the endoleak (Figure 13b).

The profile of dynamic pressure on the outlets for both cases with and without the endoleak was flat when compared with the endoleak outflow. The highest value of dynamic pressure appeared for the stent-grafts with the endoleak only inside the endoleak (Figure 14). In this part the highest fluctuation of dynamic pressure was observed due to small dimension and high blood velocity inside the calculated domain. The remaining part of the stent-graft each time had smaller dynamic pressure compared with the case without endoleak. The highest value appeared for the stent-grafts without the endoleak and was equal to 8148 ± 266Pa. For

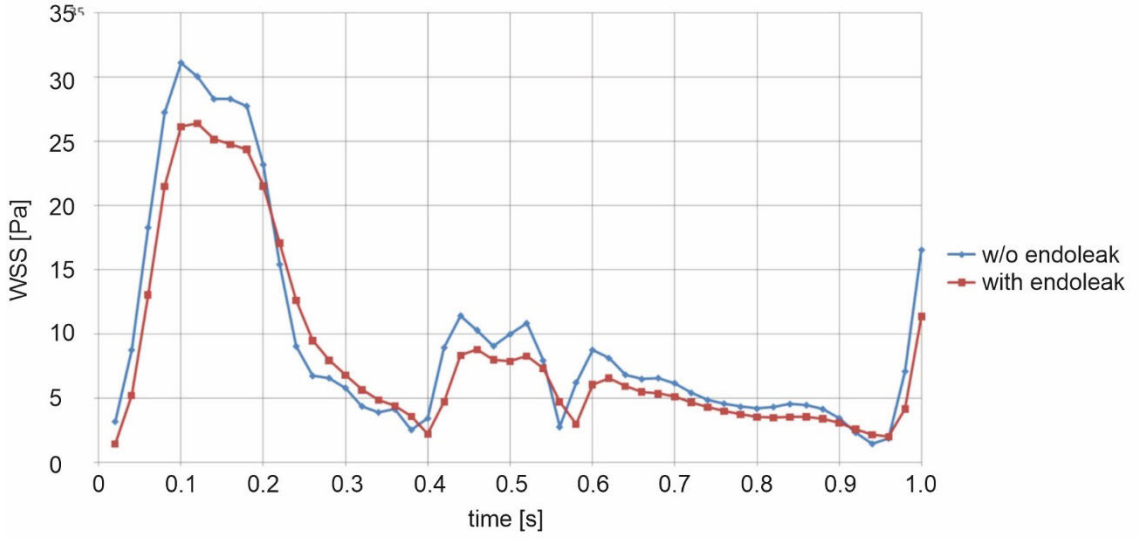

FIGURE 18. An example of wall shear stress curves for stent-graft without endoleaks (w/o endoleak) and with the endoleaks (with endoleak).

endovascular prosthesis with the endoleak about 2 times smaller dynamic pressure of 4257 ± 226Pa was observed.

Spatial distribution of WSS for the investigated endovascular prostheses showed differences during 1 second of calculation time. Curves representing average WSS for both cases with (Figure 15a) and without the endoleak (Figure 15b) each time indicated higher value at the outlets for stent-graft without the endoleak. Higher value of WSS may lower the probability of thrombosis and the appearance of higher forces that act on the stent-graft's wall, which may have protective role [8]. The maximum average WSS appeared at about 3.16 second for both cases with and without the endoleak for both bifurcation branches. For the left branch outflow without the endoleak it was about 2.19Pa and dropped to 1.80Pa in the case of with endoleak. Meanwhile, a higher drop in WSS was noticed in the right branch where the WSS values dropped from 2.15Pa in the case without the endoleak to 0.18Pa in the case without endoleak.

The Pplates representing the endoleak had smaller value of WSS compared to outlets of the stent-graft's bifurcated part (Figure 16). Near the endoleak there appeared higher values of WSS which were related to outflow presence on the stent-graft's wall. During blood flow near the endoleak there was higher shear stress, which could decreased the probability of blood coagulation as described by [23].

Our results presented that each time the value of WSS near the endoleak was higher compared to outflows of the stent-graft's bifurcated part (Figure 17). Small cross-section of the endoleak and high blood velocity increased the forces which acted on the aorta's wall near the endolek. Over and under endoleak the highest value of WSS of about 60Pa appeared. In the middle of endoleak's outflow the value of WSS was equal to 0Pa because this part has no resistance and free blood flow could occur there. The comparison of WSS near the endoleak with the outflows of stent-graft's bifurcated part showed around 3 times higher value that may decrease the possibility of blood coagulation process.

The average value of WSS of stent-graft's wall for both cases with and without the endoleak differed. The highest average value for the endovascular prosthesis without the endoleak was 32 ± 1.5Pa (Figure 18), and for the endoleak it decreased to 27 ± 1Pa.

C. WALL SHEAR STRESS (WSS)

IV. DISCUSSION

Despite optimal medical management, patients at which develop aneurysmal degeneration are discharged without intervention [15]. Our previous results showed that deformation in bifurcation part of a stent-graft may additionally disturb blood hemodynamic, leading to an increase in the WSS values and higher risk of stent-graft migration [8]. Moreover, the obtained results indicated that tortuosity and angular bends of a stent-graft were the most important parameters for appearance of a thrombus. Even with small values of tortuosity and angular bends in the iliac part of the prosthesis thrombus were restored in 22% to 31% of cases. It indicates that these parameters are dominant for thrombus appearance [3]. Furthermore, literature from the analyzed field indicates that endoleaks (type I and III) have higher risk of aneurysm rupture due to rapid sac expansion, while endoleaks (type II, IV and V) have a relatively benign course [32]. Proper planning and appropriate selection of stent-graft can prevent most of these endoleaks. In this study, we analyzed an effect of the endovascular treatment of the AAA to predict its outcome in the context of type II endoleaks appearance. Computational model of blood hemodynamics together with USG-Doppler data allowed investigation of blood velocity, blood pressure and WSS distribution. It was observed that type II endoleaks pressurize the aneurysm sac non-uniformly [33]. Moreover, *in vivo* and *ex vivo* studies

have shown that the pressure in the aneurysm sac reduces displacement forces on the stent-graft [34]. While, Li *et al.* described that a variety of clinical and experimental studies have shown that endoleaks would cause the pressure increase in AAA sac and consequently induce AAA re-enlargement and rupture [20]. Moreover, it was generally accepted that type 2 endoleaks, which do not lead to a remarkable increase of aneurysm sac, should be managed conservatively [35]. Furthermore, type 2 endoleaks are not prone to lead to major adverse events, especially to rupture [36]. While, Figueroa and Zarins observed that aortic neck dilation and Type Ia endoleaks have been associated with excessive device oversizing [37]. Analysis of different stent-graft's geometries enabled us to estimate changes in blood hemodynamic on the value of stresses formed in the region of proximal fixation as well as endoleaks appearance. It was recently described that changes in blood hemodynamic influence stent-graft's stable location [38]. It was also observed that an ideal stent-graft should have smaller porosity, higher pore density, and higher strut angle [39]. Moreover, Lu *et al.* observed that endoleak location agrees well with the peak wall stress location [2].

Until now, obtained medical data confirm the accuracy of the developed mathematical models. On this basis, we assume that aneurysms with a similar spatial configuration, may reflect the real blood hemodynamic. Nevertheless, one should remember that there may appear unusual cases which cannot be analyzed by the algorithm with satisfactory accuracy. Therefore, only thorough analysis of vast number of cases, will allow to identify outliers and take into account their specificity. According to this, we assume that the methodology proposed in this study is correct, and is in agreement with our previous data [16], [22].

Limitation to the Study: The benefits of CFD must be viewed in the context of known limitations of this approach. First, this study is limited by its retrospective nature. Second, the sample size was relatively small, and most analyses included cohort of less than 30 patients. Moreover, simulations may not be that specific to the individual patient in whom aortic appearance depend on a host of factors including genetic predisposition, lifestyle, or medication. Therefore, integration of patient-specific data should be addressed in the future.

V. CONCLUSION

Application of CFD simulations to reconstruct blood flow in clinical conditions in the circulatory system achieved an average of 98.5% and 98.7% accuracy for CFD results compared to USG-Doppler before and after surgery, respectively.

A high value of blood velocity in the endoleak may provoke its slowly rupture what can increase blood flow to the aneurysm sack. Moreover, the appearance of an endoleak reduces the average blood velocity in the whole stent-graft which in some cases may contribute to blood clotting. In addition, no clot can form at the site of the endoleak due to the high value of the wall shear in the vicinity of the leak, which prevents thrombosis.

REFERENCES

[1] N. Sakalihasan, J. B. Michel, A. Katsargyris, H. Kuivaniemi, J. O. Defraigne, and A. Nchimi, "Abdominal aortic aneurysms," *Nature Rev. Disease Primers*, vol. 4, p. 22, Nov. 2018.
[2] Y.-H. Lu, K. Mani, B. Panigrahi, W.-T. Hsu, and C.-Y. Chen, "Endoleak assessment using computational fluid dynamics and image processing methods in stented abdominal aortic aneurysm models," *Comput. Math. Methods Med.*, vol. 2016, pp. 1–9, Oct. 2016.
[3] A. Polanczyk, A. Piechota-Polanczyk, and L. Stefanczyk, "A new approach for the pre-clinical optimization of a spatial configuration of bifurcated endovascular prosthesis placed in abdominal aortic aneurysms," *PLoS ONE*, vol. 12, no. 8, Aug. 2017, Art. no. e0182717.
[4] A. Polanczyk, M. Podgorski, M. Polanczyk, N. Veshkina, I. Zbicinski, L. Stefanczyk, and C. Neumayer, "A novel method for describing biomechanical properties of the aortic wall based on the three-dimensional fluid-structure interaction model," *Interact. CardioVascular Thoracic Surg.*, vol. 28, no. 2, pp. 306–315, Feb. 2019.
[5] Z. Li and C. Kleinstreuer, "Analysis of biomechanical factors affecting stent-graft migration in an abdominal aortic aneurysm model," *J. Biomech.*, vol. 39, pp. 2264–2273, Jan. 2006.
[6] F. Lareyre, C. Mialhe, C. Dommerc, A. Mbeutcha, and J. Raffort, "Endovascular aneurysm sealing as an alternative for the treatment of failed endovascular aneurysm repair," *Vascular*, vol. 28, no. 3, pp. 251–258, Jun. 2020.
[7] F. J. Veith, R. A. Baum, T. Ohki, M. Amor, M. Adiseshiah, J. D. Blankensteijn, J. Buth, T. A. Chuter, R. M. Fairman, G. Gilling-Smith, and P. L. Harris, "Nature and significance of endoleaks and endotension: Summary of opinions expressed at an international conference," *J. Vascular Surg.*, vol. 35, pp. 1029–1035, May 2002.
[8] A. Polanczyk, M. Podyma, L. Trebinski, J. Chrzastek, I. Zbicinski, and L. Stefanczyk, "A novel attempt to standardize results of CFD simulations basing on spatial configuration of aortic stent-grafts," *PLoS ONE*, vol. 11, no. 4, Apr. 2016, Art. no. e0153332.
[9] A. Polańczyk, M. Podyma, L. Stefańczyk, and I. Zbiciński, "Effects of stent-graft geometry and blood hematocrit on hemodynamic in abdominal aortic aneurysm," *Chem. Process Eng.*, vol. 33, no. 1, pp. 53–61, Mar. 2012.
[10] B. C. Campbell, S. Christensen, C. R. Levi, P. M. Desmond, G. A. Donnan, and S. M. Davis, "Comparison of computed tomography perfusion and magnetic resonance imaging perfusion-diffusion mismatch in ischemic stroke," *Stroke*, vol. 43, pp. 2648–2653, Oct. 2012.
[11] R. Erbel, "[Aortic diseases: Modern diagnostic and therapeutic strategies]," *Herz*, vol. 43, pp. 275–290, May 2018.
[12] I. S. Rogers, D. Banerji, E. L. Siegel, Q. A. Truong, B. B. Ghoshhajra, T. Irlbeck, S. Abbara, R. Gupta, R. J. Benenstein, G. Choy, L. L. Avery, R. A. Novelline, F. Bamberg, T. J. Brady, J. T. Nagurney, and U. Hoffmann, "Usefulness of comprehensive cardiothoracic computed tomography in the evaluation of acute undifferentiated chest discomfort in the emergency department (CAPTURE)," *Amer. J. Cardiol.*, vol. 107, no. 5, pp. 643–650, Mar. 2011.
[13] G. X. Wang, S. S. Hedgire, T. Q. Le, J. D. Sonis, B. J. Yun, M. H. Lev, A. S. Raja, and A. M. Prabhakar, "MR angiography can guide ED management of suspected acute aortic dissection," *Amer. J. Emergency Med.*, vol. 35, no. 4, pp. 527–530, Apr. 2017.
[14] T. Hirano, "Searching for salvageable brain: The detection of ischemic penumbra using various imaging modalities?" *J. Stroke Cerebrovascular Diseases*, vol. 23, pp. 795–798, Jun. 2014.
[15] E. K. Shang, D. P. Nathan, R. M. Fairman, J. E. Bavaria, R. C. Gorman, J. H. Gorman, and B. M. Jackson, "Use of computational fluid dynamics studies in predicting aneurysmal degeneration of acute type B aortic dissections," *J. Vascular Surg.*, vol. 62, no. 2, pp. 279–284, Aug. 2015.
[16] A. Polanczyk, A. Piechota-Polanczyk, L. Stefanczyk, and M. Strzelecki, "Spatial configuration of abdominal aortic aneurysm analysis as a useful tool for the estimation of stent-graft migration," *Diagnostics*, vol. 10, p. 19, Oct. 2020.
[17] A. Polanczyk, M. Podgorski, T. Wozniak, L. Stefanczyk, and M. Strzelecki, "Computational fluid dynamics as an engineering tool for the reconstruction of hemodynamics after carotid artery stenosis operation: A case study," *Medicina*, vol. 54, no. 3, p. 42, Jun. 2018.
[18] Z. Tyfa, D. Obidowski, P. Reorowicz, L. Stefanczyk, J. Fortuniak, and K. Jozwik, "Numerical simulations of the pulsatile blood flow in the different types of arterial fenestrations: Comparable analysis of multiple vascular geometries," *Biocybern. Biomed. Eng.*, vol. 38, pp. 228–242, Jan. 2018.

[19] M. E. Casciaro, J. Dottori, S. El-Batti, J.-M. Alsac, E. Mousseaux, I. Larrabide, and D. Craiem, "Effects on aortoiliac fluid dynamics after endovascular sealing of abdominal aneurysms," *Vascular Endovascular Surg.*, vol. 52, no. 8, pp. 621–628, Nov. 2018.

[20] J. Li, X. Tian, Z. Wang, J. Xiong, Y. Fan, X. Deng, A. Sun, and X. Liu, "Influence of endoleak positions on the pressure shielding ability of stent-graft after endovascular aneurysm repair (EVAR) of abdominal aortic aneurysm (AAA)," *Biomed. Eng. OnLine*, vol. 15, no. S2, p. 135, Dec. 2016.

[21] A. Polanczyk, A. Piechota-Polanczyk, I. Huk, C. Neumayer, and M. Strzelecki, "Computational fluid dynamic technique for assessment of how changing character of blood flow and different value of hct influence blood hemodynamic in dissected aorta," *Diagnostics*, vol. 11, no. 10, p. 1866, 2021.

[22] A. Polanczyk, A. Piechota-Polańczyk, L. Stefanczyk, and M. Strzelecki, "Shape and enhancement analysis as a useful tool for the presentation of blood hemodynamic properties in the area of aortic dissection," *J. Clin. Med.*, vol. 9, no. 5, p. 1330, May 2020.

[23] A. Polanczyk, M. Podyma, L. Stefanczyk, W. Szubert, and I. Zbicinski, "A 3D model of thrombus formation in a stent-graft after implantation in the abdominal aorta," *J Biomech*, vol. 48, pp. 425–431, Feb. 2015.

[24] D. Jodko, D. Obidowski, P. Reorowicz, and K. Jozwik, "Blood flows in end-to-end arteriovenous fistulas: Unsteady and steady state numerical investigations of three patient-specific cases," *Biocybern. Biomed. Eng.*, vol. 37, no. 3, pp. 528–539, 2017.

[25] S. Lehoux, Y. Castier, and A. Tedgui, "Molecular mechanisms of the vascular responses to haemodynamic forces," *J. Intern. Med.*, vol. 259, pp. 381–392, Apr. 2006.

[26] A. Polanczyk, M. Podgorski, M. Polanczyk, A. Piechota-Polanczyk, L. Stefanczyk, and M. Strzelecki, "A novel vision-based system for quantitative analysis of abdominal aortic aneurysm deformation," *Biomed. Eng. OnLine*, vol. 18, no. 1, p. 56, May 2019.

[27] A. Polanczyk, T. Wozniak, M. Strzelecki, W. Szubert, and L. Stefanczyk, "Evaluating an algorithm for 3D reconstruction of blood vessels for further simulations of hemodynamic in human artery branches," in *Proc. IEEE Xplore Digit. Library*, vol. 5, Sep. 2016, pp. 103–107.

[28] A. Sun, X. Tian, N. Zhang, Z. Xu, X. Deng, M. Liu, and X. Liu, "Does lower limb exercise worsen renal artery hemodynamics in patients with abdominal aortic aneurysm?" *PLoS ONE*, vol. 10, no. 5, May 2015, Art. no. e0125121.

[29] A. Polanczyk, M. Strzelecki, T. Wozniak, W. Szubert, and L. Stefanczyk, "3D blood vessels reconstruction based on segmented CT data for further simulations of hemodynamic in human artery branches," *Found. Comput. Decis. Sci.*, vol. 42, pp. 359–371, Dec. 2017.

[30] C. Kleinstreuer, Z. Li, and M. A. Farber, "Fluid-structure interaction analyses of stented abdominal aortic aneurysms," *Annu. Rev. Biomed. Eng.*, vol. 9, no. 1, pp. 169–204, Aug. 2007.

[31] A. Polanczyk, M. Klinger, J. Nanobachvili, I. Huk, and C. Neumayer, "Artificial circulatory model for analysis of human and artificial vessels," *Appl. Sci.*, vol. 8, no. 7, p. 1017, Jun. 2018.

[32] Z. U. Rehman, "Endoleaks: Current concepts and treatments," *J. Pakistan Med. Assoc.*, vol. 71, pp. 2224–2229, Jul. 2021.

[33] N. V. Dias, K. Ivancev, T. A. Resch, M. Malina, and B. Sonesson, "Endoleaks after endovascular aneurysm repair lead to nonuniform intra-aneurysm sac pressure," *J. Vascular Surgery*, vol. 46, no. 2, pp. 197–203, Aug. 2007.

[34] S. M. Volodos, R. D. Sayers, J. P. Gostelow, and P. Bell, "Factors affecting the displacement force exerted on a stent graft after AAA repair—An *in vitro* study," *Eur. J. Vascular Endovascular Surg.*, vol. 26, no. 6, pp. 596–601, Dec. 2003.

[35] K. Patatas, L. Ling, J. Dunning, and V. Shrivastava, "Static sac size with a type II endoleak post-endovascular abdominal aortic aneurysm repair: Surveillance or embolization?" *Interactive Cardiovascular Thoracic Surg.*, vol. 15, pp. 462–466, Sep. 2012.

[36] H. S. Rayt, R. M. Sandford, M. Salem, M. J. Bown, N. J. London, and R. D. Sayers, "Conservative management of type 2 endoleaks is not associated with increased risk of aneurysm rupture," *Eur. J. Vascular Endovascular Surg.*, vol. 38, pp. 718–723, Dec. 2009.

[37] C. A. Figueroa and C. K. Zarins, "Computational analysis of displacement forces acting on endografts used to treat aortic aneurysms," *Stud. Mechanobiology, Tissue Eng. Biomater.*, vol. 73, p. 26, Sep. 2011.

[38] E. K. W. Poon, P. Barlis, S. Moore, W.-H. Pan, Y. Liu, Y. Ye, Y. Xue, S. J. Zhu, and A. S. H. Ooi, "Numerical investigations of the haemodynamic changes associated with stent malapposition in an idealised coronary artery," *J. Biomech.*, vol. 47, no. 12, pp. 2843–2851, Sep. 2014.

[39] C. H. Yu and T. K. Kwon, "Study of parameters for evaluating flow reduction with stents in a sidewall aneurysm phantom model," *Bio-Med. Mater. Eng.*, vol. 24, no. 6, pp. 2417–2424, 2014.

ANDRZEJ POLANCZYK received the Ph.D. degree in medical engineering, in 2013. He is currently a Researcher and a Team Leader at the Main School of Fire Service, Poland. He has participated in scientific grants in which he built the installation to simulate the blood flow through the abdominal section of the aorta. Recently, he received a grant funded by The National Centre for Research and Development. His research interests include biomedical, chemical, and environmental engineering.

ALEKSANDRA PIECHOTA-POLANCZYK is currently employed at the Department of Medical Biotechnology, Jagiellonian University, Kraków, Poland. Her research interests include finding of new anti-oxidative and anti-inflammatory proteins that could be potential markers and/or targets in treatment of cardiovascular diseases, as well as the role of Nrf2 and heme oxygenase 1 in cellular adaptation to oxidative stress and inflammatory reactions.

IHOR HUK received the post-graduate degree from the University of Chicago, and Heidelberg Special Training from the American Society for Parenteral and Enteral Nutrition Transplant Surgery. He was the Director of the Vascular Laboratory, Department of Surgery, MUV Medical School, where he was also a Professor of clinical surgery. Since 1984, he has performed more than 550 kidney, liver transplantation, and vascular surgeries; clinical and experimental research (SPACE-Study); and L-arginine study. He is a member of the Austrian Society of Surgery, the Austrian Society of Angiology, the Austrian Society of Vascular Surgery, the Ukrainian Academy of Higher Education, and the Ukrainian Academy of Sciences, and he also a Senate Member of the Zaporizhzhia Medical Postgraduate Academy (honoris causa).

CHRISTOPH NEUMAYER is currently the Head of the Department of Vascular Surgery, Medical University of Vienna. His research interest includes molecular mechanism of artery diseases and diabetes.

MICHAL STRZELECKI is currently employed at the Institute of Electronics, Lodz University of Technology. His scientific interests include the processing and analysis of biomedical signals and images, data analysis methods, artificial intelligence, and the development of software aimed at support of medical imaging diagnostics. Within these interests, he conducts extensive cooperation with domestic and foreign medical universities on the construction and development of systems supporting the diagnostic process.